ORIENTATION CONSTRAINTS IN DIFFUSION-LIMITED MACROMOLECULAR ASSOCIATION

The Role of Surface Diffusion as a Rate-enhancing Mechanism

OTTO G. BERG

Institute of Molecular Biology, University of Oregon, Eugene, Oregon 97403; and Department of Theoretical Physics, Royal Institute of Technology, S-10044 Stockholm, Sweden

ABSTRACT Ligand association to a reactive site on a macromolecular surface could be very slow if the site is small. The effective capture radius of the reactive site can be significantly increased if the ligand can bind weakly to the nonspecific surface around the site and then slide in a two-dimensional diffusion along the surface. In this model, the diffusion along the surface has to be properly coupled with the free diffusion in solution and the effective bimolecular association rate constant to the reactive site can be calculated as a function of the nonspecific affinity. This is carried out both for a plane and spherical surface, modeling the association to a membrane receptor or to the catalytic site on an enzyme. The result of these calculations can be used to assign reasonable values to the parameters in the quasichemical approximation of K. Solc and W. H. Stockmayer (1973, *Int. J. Chem. Kinet.*, 5:733–752). In this way a simple analytical expression can be derived for the diffusion-limited association rate constant of two asymmetrically reactive molecules, with or without surface diffusion contributing.

INTRODUCTION

Many biological processes involve the binding of ligands to specific sties on large macromolecules or macromolecular complexes. Typical examples are the following: substrate binding to the catalytic site of an enzyme, regulatory protein binding to DNA, hormone binding to membrane receptors, etc. In general, ligands will find their target sites by diffusion. If binding is dependent on a very precise alignment of the reacting molecules, the target would be very small and the association process correspondingly slow. However, for many enzymes where the catalytic region constitutes only a small fraction of the surface, substrate association still can take place at very high rates (e.g., Fehrst, 1977) as though a much larger fraction of the enzyme were the target.

There are several different ways that a diffusion-limited association could be speeded up. First it should be stressed, however, that alignment or orientation constraints are not quite as severe as might first be thought: although they can drastically reduce association rates, this reduction is not equal to the required fraction of angular orientation space. Rather, the diffusion equation allows the molecules to try many orientations in repeated encounters before diffusion carries the reactants apart. To describe this properly one must consider the diffusion in a full coordinate space, which includes the orientational coordinates (Solc and Stockmayer, 1971, 1973; Schmitz and Schurr, 1972; Schurr and Schmitz, 1976; Hill, 1975; Shoup et al., 1981).

One way of further reducing the influence of the orientation constraints would then be to introduce nonspecific forces that could hold the reactants together for a longer time while they are allowed to seek out their correct orientations. Thus, Chou and Jiang (1974) described the diffusion onto a small surface patch on a spherical molecule with an attractive potential all around it. A similar model has been presented by Zhou (1979), who takes into account the attractive interaction and the influence from the heterogeneous surface reactivity only in a thin spherical shell around the target molecule. In this way, the interaction required to hold the reactants together long enough for them to find the reactive site can be estimated. Both of these models indicate that the short range van der Waals' force could provide sufficient interaction to overcome the orientational constraint of the target molecule. For a recent discussion of these and some other models for heterogeneous surface reactivity see also Chou and Zhou (1982).

Bloomfield and Prager (1979) proposed a similar mechanism to explain the accelerated association of tail fibers on bacteriophage T4 in the presence of whiskers. These whiskers were proposed to hold the tail fiber while it was searching for its correct orientation for attachment. Bloomfield and Prager (1979) calculated the effective

Dr. Berg's present address is the Institute of Molecular Biology, University of Oregon, Eugene, OR 97403.

reorientation rate as a function of the orientational constraint and found that the overall association rate could be increased several orders of magnitude if the whisker could hold the tail fiber for a sufficiently long period.

An analogous situation exists for the association of regulatory proteins to DNA, where it was found (Riggs et al., 1970) that the association of the *Escherichia coli lac* repressor to its operator site is much faster than given by the diffusion onto a small site. Richter and Eigen (1974) explained this by proposing that the repressor could slide in a one-dimensional diffusion along the nonspecific DNA flanking the operator site. In this way the effective target size would be extended and the spatial constraints relaxed. Further theoretical analysis (Berg et al., 1981) and experimental investigation (Barkley, 1981; Winter et al., 1981) have confirmed that nonspecific sliding is indeed a rate-enhancing mechanism for the *lac* repressor. Winter et al. (1981) have also suggested a plausible molecular model for this sliding motion.

Here we shall focus on the corresponding sliding model in two dimensions, describing surface diffusion onto a reactive patch on a spherical molecule (e.g., an enzyme) or on a plane surface (e.g., a membrane). In contrast to the model of Chou and Jiang (1974), which introduces a potential well outside the surface where diffusion is as fast as in solution, we shall assume that surface binding is a discrete nonspecific binding step. This assumption takes the short-range interactions into account and makes it possible to include in the model both target rotations and a reduced mobility for ligands associated with the surface. During the nonspecific binding event, the ligands are free to move in a two-dimensional surface diffusion, until they either reach the binding site or dissociate again. In the latter case the process starts over, but the dissociated ligand then starts with very strong spatial correlations to the reactive site. In the calculations below, these spatial correlations are accounted for by an explicit coupling between the surface diffusion and the free diffusion. This leads to marked differences from the model by Bloomfield and Prager (1979), who treat the surface diffusion (or reorientation) as a totally independent step.

Thus, in the following we calculate the effective association rate constant to a surface patch on a spherical or plane surface as a function of the (nonspecific) surface affinity and for various sizes of the surface patch. For the *lac* repressor, this affinity dependence provided a very good handle for the experimental verification of the one-dimensional sliding mechanism; since the nonspecific DNA binding of the *lac* repressor is largely electrostatic, it could be varied over a wide range through variations in salt concentration. It is to be expected that nonspecific binding to biological membranes would also be largely electrostatic and amenable to experimental manipulation in the same way.

Furthermore, we show that the inverse of the effective association rate constant is essentially a linear function of bulk viscosity whether a surface diffusion mechanism operates or not. This contradicts a recent suggestion by Hasinoff (1982) that the unusual viscosity dependence of the kinetics of acetylcholinesterase indicates the presence of surface diffusion.

Finally, we discuss the association between two molecules with localized reactive patches on them. Solc and Stockmayer (1973) proposed a quasichemical approximation to describe this situation. The present results can be used to assign geometric expressions to the parameters of their model. Thus, we arrive at a simple analytical expression for the diffusion limited association rate constant between two asymmetrically reactive spheres. When surface diffusion, or reorientation within a nonreactive complex, contributes, the result is strongly dependent on the strength of the nonspecific binding. Sommer et al. (1982) investigated the reaction between small surface sites on proteins and found that the speed of the reaction required extensive reorientation during nonreactive encounters. Their results are discussed further in light of the present model.

It can be expected that surface diffusion is a very general feature in macromolecular association (and dissociation) reactions. On a small scale, it is simply the ability for reacting molecules to be held in an encounter complex while rearrangements in orientation or alignment of reacting groups take place. On a larger scale, it can produce the dramatic rate increases found for the *lac* repressor in vitro, where the effective target size is increased several orders of magnitude as surface sliding extends over long distances.

FORMULATION OF THE MODEL

The model describes the association of a ligand to a reactive patch on a spherical molecule (see Fig. 1). This reactive patch could be the catalytic site on an enzyme or some other type of ligand-binding site on a spherical macromolecule. In the limit when the spherical molecule becomes infinitely large, it will approach a plane surface. In this limit one can think of the reactive patch as a binding site on a membrane.

A ligand that binds to the reactive patch will be drawn out of solution. Ligands can also bind reversibly to other parts of the spherical surface and diffuse along the surface until they find the reactive patch or dissociate again. In this way, surface diffusion will effectively extend the size of the target, since ligands landing sufficiently close to the reactive patch on the surface will be able to slide onto it before dissociation.

We shall derive the effective association rate constant from a standard steady state analysis and follow rather closely the treatment of the corresponding one-dimensional problem (Berg and Ehrenberg, 1982). The major feature is the proper coupling between the two-dimensional diffusion along the surface and the three-dimensional diffusion in solution. This is achieved with a boundary-condition rela-

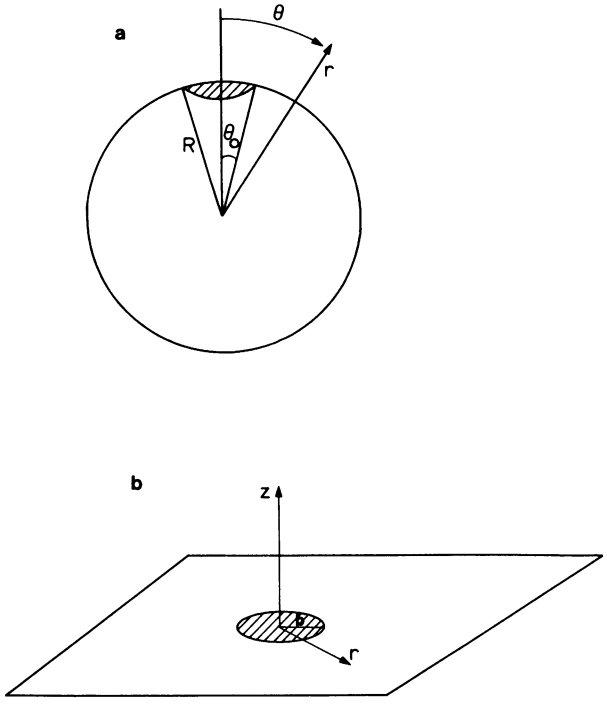

FIGURE 1 The two geometries described in the text are shown: (*a*) reactive surface patch on a spherical molecule; (*b*) circular reactive patch on an infinite plane.

tion (Eq. 3) that incorporates the required correlations; i.e., the correlations that a dissociating ligand remembers which part of the surface it just left. As we shall see in the following, this coupling is even more crucial for the two-dimensional sliding than for the one-dimensional one where it was introduced (Berg and Blomberg, 1976).

At steady state, $c(r, \theta)$ is the concentration of free ligands in solution at distance r from the center of the target molecule and at angle θ away from the center of the reactive patch (see Fig. 1). Similarly, $u(\theta)$ is the density (per unit area) of ligands nonspecifically bound at the surface of the target molecule. These distributions satisfy the stationary diffusion equation in solution

$$\frac{D}{r^2}\frac{\partial}{\partial r}\left(r^2\frac{\partial c}{\partial r}\right) + \left(D_R + \frac{D}{r^2}\right)\frac{1}{\sin\theta}\frac{\partial}{\partial\theta}\left(\sin\theta\frac{\partial c}{\partial\theta}\right) = 0; r > R \quad (1)$$

and for surface diffusion outside the reactive patch

$$\frac{D_s}{R^2\sin\theta}\frac{d}{d\theta}\left(\sin\theta\frac{du}{d\theta}\right) + \phi(\theta) = 0; \theta > \theta_o. \quad (2)$$

Here, D is the relative translational diffusion constant; i.e., D is the sum of the diffusion constants for a free ligand and for the target sphere. D_R is the rotational diffusion constant of the target sphere and D_s is the diffusion rate along the surface for ligands that are nonspecifically bound. Since D_s is a relative diffusion constant, it is determined both by the translational diffusion of the ligands along the surface and the rotational diffusion of the target sphere.

These diffusion equations are coupled at the boundary by the requirement that the net flux, $\phi(\theta)$, of ligands onto the surface equals the difference between on and off fluxes

$$\phi(\theta) \equiv D\frac{\partial c}{\partial r}\bigg|_{r=R} = \kappa c(R, \theta) - \lambda u(\theta). \quad (3)$$

κ is a local reactivity per unit area for nonspecific association to the surface, and λ is the corresponding local dissociation rate constant. At equilibrium their ratio defines the nonspecific binding constant per unit area. Thus, the nonspecific binding constant per target sphere would be

$$K \equiv 4\pi R^2\kappa/\lambda \quad (4)$$

if the whole surface is nonspecifically binding.

The steady state flux is calculated by requiring that the concentration is constant at large distances from the target

$$c(r, \theta) \xrightarrow[r\to\infty]{} c_o. \quad (5)$$

Ligands will be drawn out of solution when they reach the reactive patch either directly from solution or via surface diffusion from neighboring parts of the surface. Total absorption is achieved by requiring

$$u(\theta) \equiv 0; \theta \le \theta_o. \quad (6)$$

Then the absorption flux via surface diffusion is from Eq. 2

$$\phi_s \equiv 2\pi R^2\int_{\theta_o}^{\pi}\sin\theta\,\phi(\theta)\,d\theta = 2\pi D_s\sin\theta_o\frac{du}{d\theta}\bigg|_{\theta_o+} \quad (7)$$

and the flux directly out of solution is from Eqs. 3 and 6

$$\phi_d \equiv 2\pi R^2\int_0^{\theta_o}\sin\theta\,\phi(\theta)\,d\theta = 2\pi R^2\kappa\int_0^{\theta_o}\sin\theta\,c(R, \theta)\,d\theta. \quad (8)$$

In this way, it is assumed that the direct association onto the reactive patch is governed by the same local reactivity, κ, as the nonspecific association elsewhere on the surface. Thus, κ represents an activation barrier for the final step of bringing the molecular surfaces together. In a more general picture, this activation barrier could vary strongly over the surface, in particular between the nonspecific surface and the reactive patch. However, here we focus explicitly on the diffusion-controlled limit, immediate reaction upon contact, so that $\kappa \to \infty$ both for the specific and nonspecific association and any difference between them becomes immaterial.

The distinction of the reactive patch in the model is only given by the absence of dissociation via Eq. 6.

The effective association rate constant, k_a, is defined by

$$k_a c_o \equiv \phi_{tot} \equiv \phi_s + \phi_d. \quad (9)$$

This completes the mathematical formulation of the spherical problem. An approximate solution is derived in Appendix A. The approximations are based on the same assumptions that Shoup et al. (1981) showed to be reasonable for the case without surface sliding: (*a*) the direct association flux onto the reactive patch out of solution is homogeneous over the patch; (*b*) the absorbing boundary condition, Eq. 6, is assumed to be valid on the average over the patch. Note that these approximations will become even better when surface sliding contributes. This is because the sliding effectively extends the influence of the reactive patch, thereby reducing concentration inhomogeneities at its borders. In the limit when surface sliding over the entire sphere is dominant, the approximations in fact become exact. In Appendix B we formulate and solve the problem in the same way when the reactive site is embedded in a plane surface with surface sliding.

In the following sections we shall first look at the results in some special limits before going into the details of the general solution. Although the mathematics of the model calculations can be carried out fairly exactly, the physical picture is not so clear cut since the parameters and geometry of the interactions will not be known with any precision. Therefore, the emphasis will be on the dominant behavior of the association rate constant when the various physical parameters are changed. The approximations that are given to show this behavior more clearly are not strictly mathematical ones but were found numerically to agree well with the general expressions. For simplicity and to avoid inserting Avagadro's number in the equations, all association rate constants are assumed to be given in units $cm^3\ s^{-1}$, and all binding constants in units cm^3 (except where otherwise stated).

LIMITING RESULTS

All results are expressed in terms of the dimensionless parameters α, β, and γ defined by Eq. A6d in Appendix A. Their physical meaning can be explained as follows: $\gamma \equiv D_R R^2/D$ describes the influence of the rotational motions of the target sphere. Since the reaction radius R is the sum of the radius r_A of the target molecule and the radius r_B of the ligand, and $D_R/D = (3/4r_A^3)/(1/r_A + 1/r_B)$ from the Stokes-Einstein relations (assuming stick boundary conditions) so that

$$\gamma = \frac{3}{4}(r_B/r_A)\,(1 + r_B/r_A) \tag{10}$$

is a geometric factor. The model we are using is best applicable for small ligands and a large target molecule ($r_A \gg r_B$), and then γ will be small.

$\beta \equiv D/\kappa R$ describes the departure from diffusion control for the nonspecific binding due to a reaction step. If, as is most common in the literature of partially diffusion-controlled association, the surface reactivity

$$k \equiv 4\pi R^2 \kappa \quad (cm^3 s^{-1}) \tag{11}$$

per target sphere is used, then

$$\beta = 4\pi RD/k. \tag{12}$$

The third parameter, finally, is

$$\alpha \equiv D_s\kappa/D\lambda R = (D_s/R^2)(K/4\pi RD), \tag{13}$$

which describes the influence from the surface sliding. Here the nonspecific binding constant K for the target sphere has been introduced from Eq. 4. Since

$$k_A \equiv \frac{4\pi RD}{1 + 4\pi RD/k} \quad (cm^3 s^{-1}) \tag{14}$$

is the partially diffusion-controlled association rate constant to the whole target sphere,

$$k_D \equiv \frac{4\pi RD/K}{1 + 4\pi RD/k} \quad (s^{-1}) \tag{15}$$

is the macroscopic dissociation rate constant for nonspecific binding to the sphere. While the microscopic (or local) dissociation with rate λ only releases the ligand into solution very close to the surface, the macroscopic dissociation with rate k_D also includes diffusional separation (cf. Berg, 1978). Thus, the parameter combination

$$\alpha(1 + \beta) = D_s/R^2 k_D \tag{16}$$

is the ratio of the rate of surface diffusion (D_s/R^2) to the macroscopic rate of nonspecific dissociation. As it turns out, it is this parameter combination that is most useful to gauge the influence of the surface diffusion.

Some interesting limits can be checked explicitly (*a*) In the limit when there is no surface sliding, $D_s = 0$, $\alpha = 0$, and from Eq. A15)

$$\frac{4\pi DR}{k_a} = 1 + \frac{2\beta}{1 - x_o} - \frac{1}{(1 - x_o)^2} \sum_{n=1}^{\infty} \frac{[P_{n-1}(x_o) - P_{n+1}(x_o)]^2 K_{n+1/2}(\gamma_n)}{(2n + 1)[nK_{n+1/2}(\gamma_n) - \gamma_n K_{n+3/2}(\gamma_n)]}, \tag{17}$$

where $x_o \equiv \cos\theta_o$, $\gamma_n \equiv n(n + 1)\gamma$, P_n is a Legendre polynomial, and $K_{n+1/2}$ is a modified Bessel function. Note that without noticeable loss of accuracy, the Bessel functions can be replaced by using the approximate relation given in Eq. A8b. In the diffusion-controlled limit ($\beta = 0$), the numerical evaluation of Eq. 17 can be approximated (with an error of ~10% or less) as

$$k_a \approx 4\pi DR \frac{[(1 + \gamma)/2]^{1/2} + \sin(\theta_o/2)\cos(\theta_o/2)}{[(1 + \gamma)/2]^{1/2} + \cot(\theta_o/2)}, \tag{18a}$$

or when $\gamma \ll 1$ (with less than a factor 1.6 error for $\theta_o \to 0$ and much better elsewhere)

$$k_a \approx 4\pi DR \sin(\theta_o/2). \tag{18b}$$

That is, even without surface sliding the steric constraint enters only as the square root of the fraction, $\sin^2(\theta_o/2)$, of surface that is reactive. If all collisions were uncorrelated, the result would have been $k_a = 4\pi DR \sin^2(\theta_o/2)$. The faster association given by Eqs. 17–18 is due to the repeated encounters allowed by the diffusion equation. Once the ligand has reached the target molecule, it will bounce around many times trying out different orientations before diffusion again carries the ligand far enough away so that it loses its correlations. Another way of looking at Eq. 18b is, of course, to consider $R \sin(\theta_o/2)$ as a representation of the size of the effective target, i.e., roughly the size of the reactive patch as expected on geometric grounds. Eq. 17 agrees with the result given by Shoup et al. (1981), and these authors have discussed in detail its properties when the different parameters are varied. In what follows we shall focus on the influence of the surface sliding.

(*b*) When nonspecific dissociation is zero, $\lambda = 0$, $\alpha \to \infty$, and every ligand molecule reaching the surface outside the reactive patch will eventually slide onto it. From Eqs. A14 and Eqs. C1–C2 we can calculate the fraction, ψ_s, of ligand molecules reaching the reactive patch via surface sliding

$$\psi_s = (1 + x_o)/2 = \cos^2(\theta_o/2),$$

which is simply the fraction of the surface not covered by the reactive patch. Furthermore, we get from Eq. A15 in the limit $\alpha \to \infty$

$$k_a = \frac{4\pi DR}{1 + 4\pi DR/k}, \tag{19}$$

which is equal to the effective association rate constant to the whole sphere, k_A from Eq. 14, as it should be when sliding effectively extends the reactive region over the whole surface.

TWO-STEP APPROXIMATION

To better understand the details of the general expression for the association rate constant, it is instructive to consider first some approximate schemes. This will help tie together how the various physical processes contribute to the overall rate and also provide hints as to how more complicated situations can be described.

The general results, Eqs. A14–A15, can be summed explicity in the limit when surface diffusion is dominant. Thus when α is sufficiently large such that $\alpha n(n + 1) \gg C_n$ (where C_n is given by Eq. A8) for all n, one finds from Eq. A14 $\psi_s \approx (1 + x_o)/2$, and from Eq. A15

$$\frac{4\pi DR}{k_a} \approx 1 + \beta + \frac{1 + x_o}{1 - x_o}\frac{1}{2\alpha}\sum_{n=1}^{\infty}\frac{P_n(x_o)[P_{n-1}(x_o) - P_{n+1}(x_o)]}{n(n+1)} + \frac{1}{1 - x_o}\frac{1}{2\alpha}\sum_{n=1}^{\infty}\frac{[P_{n-1}(x_o) - P_{n+1}(x_o)]^2}{n(n+1)(2n+1)}.$$

The sums are given in Appendix C, Eqs. C3–C4, and the result can be expressed as

$$k_a \approx \frac{k_A}{1 - (k_D R^2/D_s)\{\cos^2(\theta_o/2) + \ln[\sin^2(\theta_o/2)]\}}, \tag{20}$$

where the nonspecific association and dissociation rate constants, k_A and k_D, from Eqs. 14 and 15 have been introduced.

This result can be compared with what one gets in a two-step approximation (Bloomfield and Prager, 1979)

$$\begin{array}{ccc} L + T & \underset{k_{-2}}{\overset{k_2}{\rightleftharpoons}} & (L + T) \\ & \searrow \quad \swarrow & \\ k_1 & LT & k_3 \end{array} \tag{21}$$

where the ligand molecules either hit the reactive patch directly (rate constant k_1) with probability $\sin^2(\theta_o/2)$, or bind nonspecifically (rate constant k_2) with probability $\cos^2(\theta_o/2)$. Once nonspecifically bound, they can either be transferred to the reactive patch with rate constant k_3, or dissociate with rate constant k_{-2}. Then, the rate constants in the scheme (Eq. 21) can be identified as: $k_1 = k_A \sin^2(\theta_o/2)$, $k_2 = k_A \cos^2(\theta_o/2)$, and $k_{-2} = k_D$. This two-step scheme, Eq. 21, is also equivalent to the quasichemical approximation of Solc and Stockmayer (1973).

At steady state one finds the effective association rate constant to the reactive patch

$$k_a = \frac{k_A[k_3/k_D + \sin^2(\theta_o/2)]}{k_3/k_D + 1}. \tag{22}$$

If the reactive patch is small, $\sin^2(\theta_o/2)$ can be neglected, and comparing Eq. 22 with Eq. 20 we can identify the effective transfer rate via surface sliding

$$k_3 = -\frac{D_s}{R^2}\frac{\cos^2(\theta_o/2)}{\cos^2(\theta_o/2) + \ln[\sin^2(\theta_o/2)]}. \tag{23}$$

This is exactly the result calculated by Bloomfield and Prager (1979) as the inverse of the mean time of reaching the reactive patch via surface diffusion. Thus, the two-step scheme used by these authors is equivalent to the approximate summation, Eq. 20, which is valid when surface diffusion is dominant.

There are two major approximations inherent in the two-step approach outlined above. First, it describes all nonspecific dissociations with the macroscopic rate constant k_D that assumes that the ligand loses all spatial correlations with the target molecule in each dissociation. However, as is true particularly in the diffusion-controlled limit, every macroscopic dissociation is preceded by a large number of microscopic dissociations that leave the ligand free in solution for only a very short time before it reassociates (cf. Berg, 1978). During this short time, the diffusional motions can change the θ-coordinate such that the ligand reassociates closer to (or farther from) the reactive patch, in effect increasing the rate of target

location. Thus, these microscopic dissociations are equivalent to the diffusion effects that, in the absence of surface sliding, produce an effective association rate constant, Eq. 18, which is larger than $k_A \sin^2(\theta_0/2)$, i.e., larger than the rate of locating the sphere times the fraction of surface that is reactive (cf., e.g., Solc and Stockmayer, 1973; Shoup et al., 1981).

Second, the effective transfer rate as given by Eq. 23 is independent of the nonspecific dissociation rate. In fact, the inverse of Eq. 23 is the mean time for a ligand starting somewhere on the surface to slide onto the reactive patch without any dissociation. Thus, this mean time will be dominated by those ligands that start on the surface relatively far away from the reactive patch. When nonspecific dissociation is fast, however, only ligands that are very close to the patch will have time to slide onto it before dissociation, and only those ligands should contribute to the effective transfer rate. In this way a fast nonspecific dissociation will trap the faster modes of the surface diffusion. Thus, the effective transfer rate will increase with increasing dissociation rate constant, although the overall association rate decreases, since there are fewer ligands that can transfer at any one time.

This is a very important aspect in the case of one-dimensional sliding, where the effective transfer rate is strongly dependent on the nonspecific dissociation rate constant (Berg et al., 1981). As it turns out, for the two-dimensional sliding discussed here, the dependence of the effective transfer rate on the nonspecific dissociation rate constant is much less crucial. The major part of the discrepancy (see Fig. 2) from the full result is caused by the neglect of diffusion coupling (the microscopic dissociations) in the independent two-step approximation, Eqs. 22–23. There is, however, a simple way to include these diffusion effects in the two-step scheme. The diffusion-limited result without surface sliding, Eq. 18a, can be generated from Eq. 22 if we set

$$k_3/k_D = [(1 + \gamma)/2]^{1/2} \tan(\theta_0/2). \quad (24)$$

Taken together with Eq. 23, a much better approximation to the diffusion-limited result including surface diffusion, Eq. A15, is afforded by using

$$k_3/k_D = [(1 + \gamma)/2]^{1/2} \tan(\theta_0/2) - (D_s/R^2 k_D)/\{1 + \ln[\sin^2(\theta_0/2)]/\cos^2(\theta_0/2)\}, \quad (25)$$

giving an error in k_a of less than ~20%. Without this improvement, the two-step approximation is not good in the limit when surface sliding contributes little to the effective association rate. Eq. 25 can also serve as a useful approximation for more complicated situations, e.g., in the quasichemical model of Solc and Stockmayer (1973) describing the association reaction between two asymmetrically reactive molecules. This is explored further in the following sections.

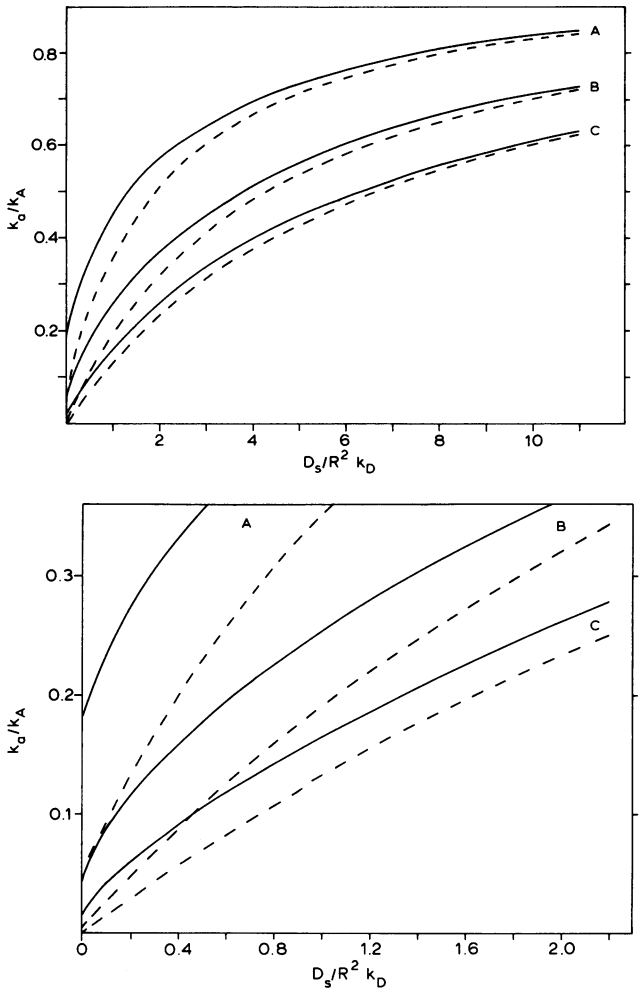

FIGURE 2 Influence of surface diffusion on the effective association rate constant calculated for various values of θ_0 and with $\beta = \gamma = 0$ as explained in the text. Solid curves are from the full result of Eq. A15; dashed curves are from the two-step approximation, Eqs. 22–23. Curves *A*: $\theta_0 = 25.8°$; curves *B*: $\theta_0 = 8.1°$; curves *C*: $\theta_0 = 2.6°$.

DEPENDENCE ON PHYSICAL PARAMETERS

The general results can easily be calculated numerically from Eq. A15, since the value of the required Legendre polynomials and Bessel functions can be generated simply with the aid of their respective recurrence relations. Note that the approximate relation (Eq. A8b) can totally do away with the Bessel functions. This simplifies the numerical calculations significantly without noticeable loss of accuracy. The results can best be represented graphically.

Although curves can be generated for all target sizes, the results for small surface sites have been emphasized in the figures. This is partially because the influence from surface diffusion can be depicted most clearly in this limit. Also, in the absence of long-range attractive forces, diffusion must carry reacting groups into very precise positions for reactions to occur. In this case, the effective target size will be

very small even if the region of physical contact (binding site) between the molecules is appreciable.

In Fig. 2 we have plotted k_a/k_A, which is the ratio of the effective association rate constant, k_a, to the reactive patch and the association rate constant, k_A, to the whole sphere. This ratio has been plotted for various sizes of the surface patch as a function of D_s/R^2k_D, which is the influence of surface diffusion from Eq. 16. The dashed lines are the corresponding results from the independent two-step approximation, Eqs. 22–23. The effective association rate constant becomes less dependent on the size of the reactive patch the more surface diffusion contributes. Also, k_a/k_A taken as a function of D_s/R^2k_D is very insensitive to the particular choice of the parameter β (the departure from diffusion control, Eq. 12), except in the limit when $D_s \ll R^2k_D$. The curves in Fig. 2 were calculated for total diffusion control ($\beta = 0$) and no rotational motions of the target ($\gamma = 0$). As surface sliding extends its influence over the whole sphere, k_a/k_A approaches 1.

In Fig. 3 we have plotted $k_a/4\pi DR$, the ratio of the effective association rate constant k_a and the diffusion-limited association rate constant for the whole sphere. This ratio has been plotted for various values of β and γ as a function of α from Eq. 13. The model we have is best applicable for a large target sphere and small ligands; then the influence of target rotation, γ from Eq. 10, will be small, and as seen in Fig. 3 will not contribute much to the effective association rate.

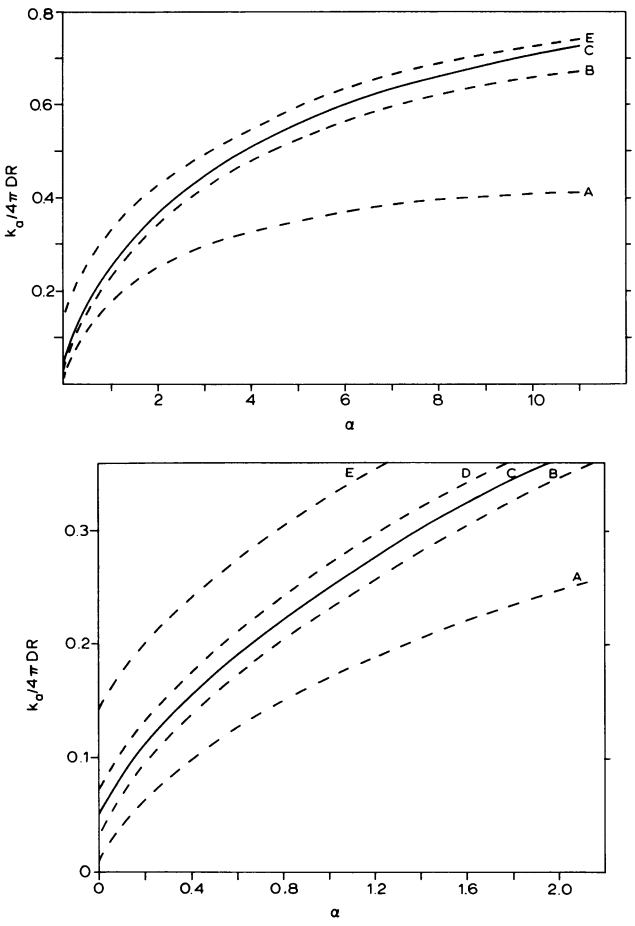

FIGURE 3 Effective association rate constant as a function of surface diffusion for various parameter values as explained in the text. $\theta_o = 8.1°$ in all cases. Curve *A*: $\beta = 1, \gamma = 0$; curve *B*: $\beta = 0.1, \gamma = 0$; curve *C*: $\beta = 0, \gamma = 0$; curve *D*: $\gamma = 1, \beta = 0$; curve *E*: $\gamma = 9, \beta = 0$.

From Fig. 2 it can be seen that a very significant increase in the effective association rate constant can be achieved with $D_s/R^2k_D = \alpha(1 + \beta)$ in the range 1 to 10. This corresponds to a nonspecific binding constant from Eq. 13, $K \equiv \alpha 4\pi R^3(D/D_s)6 \times 10^{20}$ M^{-1}, if R is in centimeters. For example, for $D/D_s = 5, \alpha = 5, \beta = 0$, and $R = 40$ Å one finds $K \sim 10^4 M^{-1}$. Thus a fairly moderate surface affinity can have a very large effect on the effective association rate if surface sliding operates.

Assuming that surface diffusion D_s has the same viscosity dependence as free diffusion D, α from Eq. 13 is viscosity independent. Then variations in viscosity will only affect the parameter $\beta \equiv 4\pi DR/k$, which should be inversely proportional to viscosity as is the diffusion constant. For uniformly reactive spheres, the association rate constant from Eq. 14 can be expressed as $k_A^{-1} = k^{-1} + (k\beta)^{-1} = k^{-1} + (4\pi DR)^{-1}$ so that k_A^{-1} plotted as a function of viscosity would be a straight line with intercept at $k_A^{-1} = k^{-1}$. The slope of the line determines the effective target radius if the diffusion rate is known. For the more complicated expressions including the orientational constraint ($\theta_o < \pi$), with or without surface diffusion, the predicted viscosity dependence can best be examined by plotting k/k_a as a function of $1/\beta$. In most cases investigated we find almost perfectly straight lines, see Fig. 4. Thus the qualitative behavior of the viscosity dependence is not changed when a more complex diffusional process is taken into account.

From Fig. 4 we can seen more quantitatively the effects of introducing surface diffusion in the sterically restricted system. If we set $1/k_a = 1/k_{eff} + 1/4\pi DR_{eff}$ in analogy with the result for uniformly reacting spheres, the straight lines in Fig. 4 can be interpreted as

$$k/k_a = k/k_{eff} + (R/R_{eff})(1/\beta). \tag{26}$$

Thus, the intercept at $1/\beta = 0$ gives the effective surface reactivity k_{eff}, and the slope gives the effective target radius, R_{eff}, for the sterically restricted system. When surface diffusion is absent ($\alpha = 0$, the dash-dot line in Fig. 4), the effective surface reactivity is a factor $\sim\sin^2(\theta_o/2)$ smaller than that for the whole sphere, and the effective target radius is $R_{eff} \sim R \sin(\theta_o/2)$ as would be expected on geometrical grounds. The linear viscosity dependence in this limit ($\alpha = 0$) agrees with what was found numerically by Schmitz and Schurr (1972). When some surface sliding is introduced ($\alpha \lesssim 0.1$, dashed lines in Fig. 4), significant curvature appears but only in a very limited range of α and β values; the main change is that the effective surface

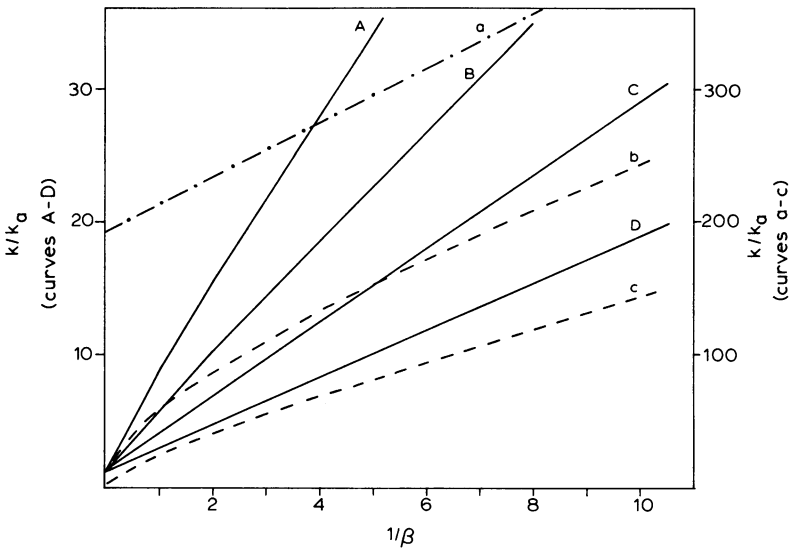

FIGURE 4 Predicted viscosity dependence of the inverse of the effective association rate constant for various extent of surface diffusion as explained in the text. $\theta_o = 8.1°$ in all cases. The dashed curves (which should be read off the scale on the right) are curve *a*: $\alpha = 0$; curve *b*: $\alpha = 0.02$; curve *c*: $\alpha = 0.1$. The solid curves (which should be read off the scale on the left) are curve *A*: $\alpha = 0.5$; curve *B*: $\alpha = 1$; curve *C*: $\alpha = 2$; curve *D*: $\alpha = 5$.

reactivity quickly approaches that of the whole sphere, while the effective target radius as defined from the slope is not altered much. Then, with increasing surface diffusion, the effective target radius increases while the effective surface reactivity remains essentially constant.

An upwards convex curvature in the viscosity dependence was also predicted by Solc and Stockmayer (1973) for surface sites with a smeared probability distribution rather than with a step-function distribution. Thus, as could be expected, surface sliding effectively smears the reactivity distribution. However, the nonlinear viscosity dependence appears only in a very limited region of small α, i.e., when surface sliding contributes little, and large β, i.e., for low viscosity when diffusion control is not total.

The model prediction that the viscosity dependence is given by the dependence on $1/\beta$ rests on two assumptions. (*a*) Surface diffusion and rotational diffusion has the same dependence on bulk viscosity as the translational diffusion. (*b*) The surface reactivity k is not viscosity dependent.

PLANE SURFACE

If we let $R \to \infty$ and $\theta_o \to 0$ while $R \sin \theta_o = b$ is kept constant, the results above would give the association rate constant to a circular surface patch of radius b embedded in an infinite plane surface. In this limit, the parameter α from Eq. 13 would be zero. A more useful parameter (also dimensionless) would be

$$\alpha' \equiv \alpha/\sin \theta_o \equiv (D_s/D)(K'/b), \tag{27}$$

where $K' \equiv \kappa/\lambda$ (in centimeters) is the nonspecific binding constant per unit surface area, see Eq. 4. In the diffusion-controlled limit ($\beta = 0$) and without surface diffusion ($\alpha' = 0$), the effective association rate constant is (Richter and Eigen, 1974; Hill, 1975)

$$k'_A = 4bD \ (\mathrm{cm^3 s^{-1}}). \tag{28}$$

Then

$$k'_D \equiv k'_A/\pi b^2 K' = 4D/\pi b K' \ (\mathrm{s^{-1}}) \tag{29}$$

will be the corresponding diffusion-limited dissociation rate constant for a nonspecific circular surface patch of radius b embedded in an infinite plane surface. Thus, the parameter α' from Eq. 27 can be expressed as

$$\alpha' = (4/\pi)(D_s/b^2 k'_D) \tag{30}$$

so that α' is the ratio of the nonspecific binding time ($\sim 1/k'_D$) and the time ($\sim b^2/D_s$) of sliding across a patch of radius b.

In the diffusion-limited case ($\beta = 0$), $k_a/4bD$ as a function of α' is a measure of the effective target extension due to surface diffusion. This has been plotted as the dashed lines in Fig. 5 for some small values of θ_o. When $\theta_o \to 0$, the curves approach the solid line, which is the result from Appendix B, Eq. B27, where the association rate constant has been calculated for the planar case. For $\alpha' \gtrsim 5$, a reasonable approximation is

$$k_a \approx 2\pi b D \alpha'/\ln \alpha' = 2\pi D_s K'/\ln(D_s K'/Db) \tag{31}$$

in the diffusion-limited case, and the association rate is determined primarily by the surface properties.

For comparison in the case of one-dimensional sliding along a cylindrical surface, the results of Berg and Ehrenberg (1982) can be approximated as $k_a \approx \pi^2 bD(2\alpha'/\ln \alpha')^{1/2}$, where α' is defined by Eq. 27 above and b is the

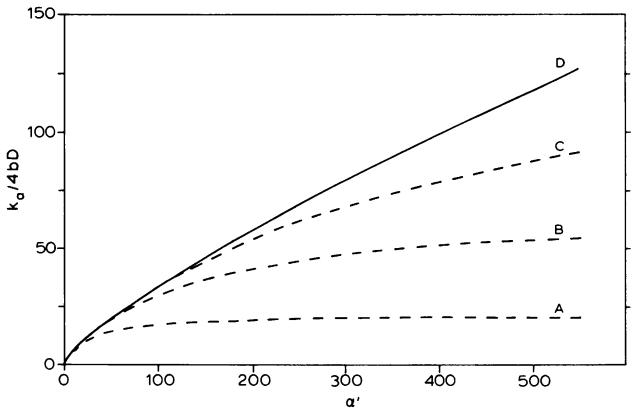

FIGURE 5 The effective target extension due to surface diffusion as explained in the text. Curve *A*: $x_0 = 0.99$ ($\theta_0 = 8.1°$); curve *B*: $x_0 = 0.999$ ($\theta_0 = 2.6°$); curve *C*: $x_0 = 0.9998$ ($\theta_0 = 1.1°$); curve *D*: result for the infinite plane of Eq. B27.

cylinder radius. Thus, the effective target extension due to surface sliding is $\sim(\alpha'/\ln\alpha')^{1/2}$ in the one-dimensional case, whereas it is $\sim\alpha'/\ln\alpha'$ in the two-dimensional case, Eq. 31. In contrast to the proposal by Richter and Eigen (1974) that the target extension would be proportional to $(\alpha')^{1/2}$ in both cases, our calculations show a fundamental difference between one- and two-dimensional sliding. This is because a plane is a much more powerful sink than a line. Thus, a ligand dissociating from the plane would not lose its spatial correlations with the reactive patch before reassociating to the plane again, and thereis no one effective dissociation rate constant from the planar surface. The parameter k'_D defined in Eq. 29 is a useful quantity to describe nonspecific dissociation, but it is not the dissociation rate from the plane; it is the dissociation rate constant from a nonspecific patch of radius b embedded in an otherwise inert plane.

Just as in the one-dimensional case (Berg and Blomberg, 1978; Berg et al., 1981), the effective association rate constant will not continue to increase indefinitely with increasing surface binding α'. When the target extension runs out of available surface k_a will level off.

The agreement in Fig. 5 between the infinite-plane result and the various spherical surfaces at intermediate and small α' demonstrate two points. First, the extension of the plane to infinity does not introduce any mathematical artifacts; as long as the available surface is larger than the effective target extension, the infinite plane is applicable. Second, also association to a site on a spherical molecule can be totally dominated by the surface properties under a wide range of physical situations.

To get a feeling for the physical requirements to produce a substantial rate enhancement, let us consider an example. From Fig. 5 it is seen that a target extension of a factor of 50 requires $\alpha' \approx 150$. From Eq. 27, this would require a nonspecific binding constant per unit surface area: $K' = 150\ bD/D_s$. Furthermore, the total surface would have to be at least $50b$ in radius to give a 50-fold extension. Thus, the total nonspecific surface binding (per target) would have to be $K_{nonsp} \geq \pi(50b)^2K'6 \times 10^{20} \approx 3 \times 10^6\ M^{-1}$ if $D/D_s \approx 5$ and $b = 10$ Å.

TWO ASYMMETRICALLY REACTIVE MOLECULES

Quasichemical Approximation

When the associating ligands are also asymmetrically reactive, the diffusion description becomes very complex. To overcome this difficulty, Solc and Stockmayer (1973) proposed a simple scheme, which they called the quasichemical approximation. In this scheme it is assumed that the association can be subdivided into independent steps of association, reorientation, and dissociation just as in the two-step approximation discussion above for one asymmetrically reactive molecule. In the diffusion-controlled limit, the effective association rate constant k_a of the quasichemical approximation can be expressed as

$$\frac{4\pi DR}{k_a} = \frac{(1 + k_D/k_\alpha)(1 + k_D/k_\beta) + (1 - \psi_A)}{\cdot\ (1 - \psi_B)/(\psi_A\psi_B + \psi_A k_\beta/k_D + \psi_B k_\alpha/k_D)} \Big/ (1 + \psi_A k_D/k_\alpha)(1 + \psi_B k_D/k_\beta), \quad (32)$$

where $\psi_A = \sin^2(\theta_A/2)$ is the fraction of the surface of an A molecule that is reactive and similarly for B. k_D is the nonspecific dissociation rate constant for unreactive A-B complexes. $k_\alpha(k_\beta)$ is the reorientation rate for an A (B) molecule in a nonspecific A-B complex to turn its reactive site towards its partner. When one of the molecules (e.g., B) is uniformly reactive, $\psi_B = 1$ in Eq. 32 and the two-step result of Eq. 22 is recovered.

The result of the previous sections now make it possible for us to identify k_α and k_β with the effective transfer rate (reorientation rate) from Eq. 25. Thus,

$$\frac{k\alpha}{k_D} = \left\{\frac{\psi_A[1 + (3r_B/4r_A)(1 + r_B/r_A)]}{2(1 - \psi_A)}\right\}^{1/2} - \frac{(D_{sA}/k_D R^2)}{1 + \ln\psi_A/(1 - \psi_A)} \quad (33)$$

and similarly for k_{β/k_D} with exchange of subscripts A and B. D_{sA} is the effective surface diffusion constant for a B molecule over the surface of A (and conversely for D_{sB}). Thus, D_{sA} would be influenced both by the rotational diffusion of the A molecule and the sliding motion of the B molecule; it is not expected to be faster than that of free diffusion

$$D_{sA} \approx R^2 D_A^{rot} + D_B = \tfrac{3}{4}(1 + r_B/r_A)^2 D_A + D_B \sim D \quad (34)$$

and similarly for D_{sB}. An exact calculation would require taking hydrodynamic interactions, surface friction, and other local potentials into account. At present, surface diffusion must be considered as an adjustable parameter,

but with a physically reasonable value. In the corresponding one-dimensional case for *lac*-repressor sliding along DNA, it was found (Winter et al., 1981) that the sliding rate was reduced less than an order of magnitude from the rate of free diffusion.

Note that Solc and Stockmayer (1973) in their results use an average rotational time τ_A (τ_B) defined as $\tau_A \equiv \psi_A/k_\alpha$ ($\tau_B \equiv \psi_B/k_\beta$). The identification suggested by Eq. 33 makes this rotational time quite different from an ordinary rotational correlation time.

Let us concentrate on the interesting case with small surface sites, $\psi_A \ll 1$ and $\psi_B \ll 1$; then one finds that $k_D\psi_A/k_\alpha \ll 1$ and $k_D\psi_B/k_\beta \ll 1$ as well, and Eq 32 simplifies to

$$\frac{4\pi DR}{k_a} = \left(1 + \frac{k_D}{k_\alpha}\right)\left(1 + \frac{k_D}{k_\beta}\right) + \frac{k_D}{\psi_A k_\beta + \psi_B k_\alpha}. \quad (35)$$

When surface diffusion is absent, $D_{sA} = D_{sB} = 0$ in Eq. 33, one finds to lowest order in θ_A and θ_B

$$k_a \approx 4\pi DR\{\sin^2(\theta_A/2)\tan(\theta_B/2) \cdot [\tfrac{1}{2} + (3r_A/8r_B)(1 + r_A/r_B)]^{1/2} + \sin^2(\theta_B/2)\tan(\theta_A/2) \cdot [\tfrac{1}{2} + (3r_B/8r_A)(1 + r_B/r_A)]^{1/2}\}. \quad (36)$$

The expression in curly brackets consequently is the steric constraint factor for small reactive sites on two spherical molecules.

We can check the consistency of Eq. 36 by a comparison with the numerical calculations of Schmitz and Schurr (1972). These authors argue that the target sites on the two molecules should be of about the same size b; i.e.,

$$b = r_A \sin\theta_A = r_B \sin\theta_B \quad (37a)$$

or for small sites

$$\theta_A = b/r_A, \qquad \theta_B = b/r_B. \quad (37b)$$

In the limit when one of the molecules is much larger than the other ($r_B \gg r_A$, and the surface of B approaches a plane), Eqs. 36 and 37 give

$$k_a = 2\pi Db\sin^2(\theta_A/2)\,[(\tfrac{1}{2})^{1/2} + (\tfrac{3}{8})^{1/2}]. \quad (38)$$

The numerical factor $(\frac{1}{2})^{1/2} + (\frac{3}{8})^{1/2} \approx 1.32$ is somewhat smaller than the numbers 1.65 to 2.23 calculated numerically by Schmitz and Schurr from a diffusion model for a similar geometric configuration. The main difference is that Schmitz and Schurr consider the reactive site on the B molecule to be protruding as a half sphere with radius b into solution, and this can also account for most of the numerical difference.

If both molecules are of equal size, $r_A = r_B$, while their reactive sites are small compared with r_A, Eqs. 36 and 37 give

$$k_a = 8\pi Db\sin^2(\theta_A/2), \quad (39)$$

which is exactly the result conjectured by Schurr and Schmitz (1976) to be valid for this case.

These agreements provide an independent control that the quasichemical approximation by Solc and Stockmayer (1973) is quite powerful even with the very simple transfer rate constants (reorientation rates) proposed above, at least when surface diffusion does not contribute. It seems likely, however, that it will remain a very good approximation also when surface diffusion is significant, just as was the case for the two-step model discussed above. Thus, Eqs. 32–33 should provide a useful analytic expression to describe a very complicated diffusional process.

RELATION TO EXPERIMENTS

As shown above, the introduction of surface diffusion in the association mechanism does not qualitatively change the predicted viscosity dependence. The inverse of the association rate constant is a linear function of viscosity (except in a very limited region of parameter values, *cf.* Fig. 4). The slope of the line provides information on the effective target radius; if this is significantly larger than the size of the reactive site, the influence of surface diffusion can be estimated. The expected linear (or possibly weaker than linear) viscosity dependence of the association rate constant, however, contradicts a recent suggestion by Hasinoff (1982) that the dependence proportional to (viscosity)$^{3/2}$ he observed for acetylcholinesterase association could signal the presence of surface diffusion. This suggestion was based in part on the erroneous conjecture by Richter and Eigen (1974) as discussed above that the effective target size would be proportional to $(D_s/k_D)^{1/2}$ for surface sliding as it is for one-dimensional sliding. Hasinoff's suggestion was also based on the untenable assumption that the nonspecific dissociation rate k_D was not diffusion controlled, while the nonspecific association rate $k_A \approx 4\pi DR$ was totally diffusion controlled; if the nonspecific binding constant $K = k_A/k_D$ is to be diffusion independent, k_A and k_D must be diffusion controlled to the same degree. Thus, if surface sliding does cause the interesting viscosity dependence observed by Hasinoff (1982), the causal link is not obvious from the model. Instead, it would require very special and unlikely properties of the surface: either the nonspecific binding is strongly dependent on solvent, or the surface sliding is impeded more drastically by an increase in bulk viscosity than is normal translational diffusion. Of course, surface sliding might still play an important role in this system.

Sommer et al. (1982) have investigated the reaction between small reactive centers on various proteins. To explain the fast rates observed, they have to assume that two proteins can be held together nonspecifically, while they are free to reorient so that their respective reactive centers can come together. This is a reaction between two equal asymmetric molecules, and we can use the results from the previous section to interpret the results. Since the

reaction sites are very small their data require that surface diffusion is dominant, and from Eq. 33 we can take

$$k_\alpha = k_\beta = (D_s/R^2)/(-1 - \ln\psi) \tag{40}$$

as the reorientation rate. From Eq. 34, the sliding rate is at most $D_s \approx 4D_A$, where D_A is the free diffusion rate of one protein molecule. The interaction radius is $R = 2r_A$ and one finds $D_s/R^2 \approx (4/3)D_{rot}$. Thus, the effective transfer rate would be at most $k_\alpha \approx (4/3)D_{rot}/(-1 - \ln\psi)$. Since Solc and Stockmayer (1973) did not assign any particular values to the rates of reorientation in their quasichemical model, Sommer et al. (1982) instead use the rotational correlation time, $\tau_{rot} = 1/6D_{rot}$, and effectively take $k_\alpha = 6\psi D_{rot}$ as a measure of the reorientation rate for a nonspecifically bound complex. Thus, these considerations lead to a lower limit of the estimated lifetimes of the nonspecific complexes that are a factor $\sim 5\psi(-1 - \ln\psi)$—(varying between 1/20 and 1/6 for their data) smaller than those derived by Sommer et al. (1982). Thus, for most of the proteins investigated by them, the lifetime of the nonspecific complex would be at least a few microseconds. Since the diffusion-limited rate of bringing the proteins together is $\sim 3 \times 10^9\ M^{-1}s^{-1}$, this would correspond to a nonspecific affinity between these proteins of $\sim 10^4\ M^{-1}$ or greater.

DISCUSSION

A reactive site embedded in a larger molecular structure can have its effective capture radius increased dramatically, if ligands can slide along the regions flanking the site. In this way the larger molecular structure can serve as a kind of antenna guiding the ligands to the reactive site, thereby also confining the diffusional search to only one or two (rather than three) dimensions (Adam and Delbrück, 1968). This idea has proven very fruitful, especially in the one-dimensional case where detailed theoretical calculations have been used for the interpretation of experimental data to confirm the existence of sliding as a rate-enhancing mechanism.

The two-dimensional surface sliding can produce rate enhancements just as dramatic as in the one-dimensional case. However, as shown above, surface sliding has properties markedly different from the linear sliding. This is due to the strong spatial correlations in the nonspecific dissociations; a ligand dissociating from the surface will remember from which part of the surface it came.

Sliding along a spherical surface can also be regarded as a molecular reorientation within an encounter complex, and is a way of overcoming orientation constraints. Again, the strong correlations in the nonspecific dissociations have to be accounted for. In the diffusion-controlled limit, this is the major source of error in the independent two-step approximation discussed above.

Note that when surface sliding contributes, the association can be governed primarily by the surface properties; even in the diffusion-controlled limit the translational diffusion rate through bulk solution can be of negligible importance for the determination of the association rate constant. Surface sliding is a local motion partially determined by rotations that are slowed down much less in vivo than is translation (Lepock et al., 1983). Thus, a diffusion-controlled rate constant measured in vitro will not necessarily be slowed down in vivo as much as the translational diffusion rate, and this could make an order-of-magnitude difference for the estimate of an association rate constant in the living cell.

Just as in the one-dimensional case, theoretical calculations elucidating how the rate enhancement depends on the molecular parameters should be useful when more experimental data becomes available. It is to be expected that two-dimensional sliding will also prove to be a rate-enhancing mechanism used in nature.

APPENDIX A

The general solution to Eq. 1 can be expressed as

$$c(r,\theta) = \sum_{n-1}^{\infty} A_n(\gamma_n r/R)^{-1/2}K_{n+1/2}(\gamma_n r/R)\,P_n(\cos\theta) + A_0/r + c_0 \tag{A1}$$

where $\gamma_n \equiv [n(n+1)\,D_R R^2/D]^{1/2}$. $K_{n+1/2}$ is a modified Bessel function and P_n is a Legendre polynomial. For the distribution of nonspecifically bound ligands on the surface, we can make the ansatz

$$\sum_{n-0}^{\infty} B_n P_n(\cos\theta) = \begin{cases} 0; & \theta \leq \theta_0 \\ u(\theta); & \theta_0 < \theta < \pi. \end{cases} \tag{A2}$$

This ansatz is always valid because of the completeness of the Legendre polynomials.

Inserting the expansions Eqs. A1 and A2 into the boundary conditions, Eq. 3, and using the orthogonality properties, Eq. C5, of the Legendre polynomials gives the following relations

$$\begin{aligned} &\int_0^\pi \sin\theta\, P_n(\cos\theta)\,\phi\,(\theta)\,d\theta \\ &\quad = (D/R)\,(n + 1/2)^{-1}(\gamma_n)^{-1/2}A_n \\ &\qquad \cdot [nK_{n+1/2}(\gamma_n) - \gamma_n K_{n+3/2}(\gamma_n)] \\ &\quad = (n + 1/2)^{-1}(\gamma_n)^{-1/2}[\kappa A_n k_{n+1/2}(\gamma_n) \\ &\qquad - \lambda(\gamma_n)^{1/2}B_n]; \qquad n \neq 0 \end{aligned} \tag{A3a}$$

and for $n = 0$

$$\begin{aligned} \phi_{tot} &\equiv 2\pi R^2 \int_0^\pi \sin\theta\phi(\theta)d\theta \\ &= -4\pi DA_0 = 4\pi R^2\kappa c_0 + 4\pi R\kappa A_0 - 4\pi R^2\lambda B_0. \end{aligned} \tag{A3b}$$

From these equations, the relation between A_n and B_n can be solved.

Inserting the ansatz Eq. A2 in the differential Eq. 2 gives

$$(D_s/R^2)\sum_{n-0}^{\infty} n(n+1)B_nP_n(\cos\theta) = \begin{cases} \phi(\theta); & \theta_0 < \theta < \pi \\ -(2\pi R^2\sin\theta_0)^{-1}\,\phi_s\delta(\theta - \theta_0); & \theta = \theta_0 \\ 0; & \theta < \theta_0. \end{cases} \tag{A4}$$

The δ-function contribution at $\theta = \theta_0$ appears because $du/d\theta$ from Eq. A2 is discontinuous at $\theta = \theta_0$ jumping from zero at $\theta = \theta_0-$ to $(du/d\theta)_{\theta_0+}$ at $\theta = \theta_0+$. The magnitude of this jump is determined from Eq. 7, which gives the surface flux ϕ_s onto the reactive patch. In this way Eq. A4 effectively extends the differential Eq. 2 to be valid over the whole surface by forcing the gradient at $\theta = \theta_0+$ to give the as yet undetermined surface flux ϕ_s.

Using the orthogonality properties of Legendre polynomials, Eq. C5, in Eq. A4, B_n can be solved for as

$$(D_s/R^2)(n + \tfrac{1}{2})^{-1}n(n + 1)B_n = \int_{\theta_0}^{\pi} \sin\theta\, P_n(\cos\theta)\, \phi(\theta) d\theta - (\phi_s/2\pi R^2)\, P_n(\cos\theta_0). \quad (A5)$$

Before continuing, let us simplify the notations and introduce dimensionless variables

$$x \equiv \cos\theta, \qquad x_0 \equiv \cos\theta_0, \quad (A6a)$$

$$\psi_s \equiv \phi_s/\phi_{tot}, \qquad \psi(x) \equiv 4\pi R^2\phi(\theta)/\phi_{tot}; \quad (A6b)$$

$$b_n \equiv B_n 4\pi D_s/\phi_{tot}; \quad (A6c)$$

$$\alpha \equiv D_s\kappa/D\lambda R, \qquad \beta = D/\kappa R, \qquad \gamma \equiv D_R R^2/D. \quad (A6d)$$

Then Eq. A5 with the aid of Eq. A3a can be expressed as

$$\frac{b_n}{\alpha} = -\frac{n + \tfrac{1}{2}}{C_n + \alpha n(n + 1)} \cdot \left[2\psi_s P_n(x_0) + \int_{x_0}^{1} P_n(x)\psi(x)dx\right]; \cdot n \neq 0 \quad (A7)$$

where

$$\frac{1}{C_n} \equiv \beta - \frac{K_{n+1/2}(\gamma_n)}{nK_{n+1/2}(\gamma_n) - \gamma_n K_{n+3/2}(\gamma_n)} \quad (A8a)$$

and

$$\gamma_n \equiv [n(n+1)\gamma]^{1/2}.$$

Numerically one finds that for all n and γ, C_n can be approximated to within a few percent by

$$1/C_n \approx \beta + 2/[1+(2n + 1)(1 + \gamma)^{1/2}]. \quad (A8b)$$

Now, Eq. A7 determines the expansion coefficients from the surface flux ψ_s and the direct absorption flux $\psi(x)$ onto the reactive patch. The surface flux onto the reactive patch is from Eq. 7

$$\psi_s = -\frac{1}{2}\sum_{n-1}^{\infty} b_n \frac{n(n + 1)}{2n + 1}[P_{n-1}(x_0-) - P_{n+1}(x_0-)] \quad (A9)$$

and the direct association flux $\psi(x)$ is to be determined from the requirement (Eq. A2)

$$\sum_{n-0}^{\infty} b_n P_n(x) = 0; \qquad x_0 \le x \le 1. \quad (A10)$$

Thus, the problem is in principle determined by Eqs. A7–A10.

Eq. A7 excludes the case $n = 0$; from Eq. A3b we can write the effective association rate constant

$$k_a \equiv \phi_{tot}/c_0 = 4\pi DR/(b_0/\alpha + 1), \quad (A11)$$

where b_0 must be determined from the other b_n and the condition in Eq. A10. One possibility is to require that this condition be valid on the average over the patch; i.e.,

$$\int_{x_0}^{1} \sum_{n-0}^{\infty} b_n P_n(x)dx = 0,$$

which gives

$$b_0 = -\frac{1}{1 - x_0}\sum_{n-1}^{\infty}\frac{b_n}{2n + 1}[P_{n-1}(x_0) - P_{n+1}(x_0)]. \quad (A12)$$

The fluxes ψ_s and $\psi(x)$ still remain to be determined. One simple approximation that works well in the case when there is no surface diffusion (Shoup et al., 1981) is to assume the direct association flux $\psi(x)$ to be homogeneous over the reactive patch (i.e., $\psi[x]$ = constant for $x_0 < x < 1$). With this approximation of the system of equations can be closed and the effective association rate constant calculated. Thus, since the total flux is conserved, Eq. A6b, we can set

$$\psi(x) = 2(1 - \psi_s)/(1 - x_0). \quad (A13)$$

Inserting this in Eq. A9 and solving for ψ_s gives

$$\frac{1}{\psi_s} = 1 + \frac{1 - x_0 + \sum_{1}^{\infty}[1 + \alpha n(n + 1)/C_n]^{-1}P_n(x_0) \cdot [P_{n-1}(x_0) - P_{n+1}(x_0)]}{1 + x_0 - (1 - x_0)^{-1}\sum_{1}^{\infty}[1 + \alpha n(n + 1)/C_n]^{-1} \cdot (2n + 1)^{-1}[P_{n-1}(x_0) - P_{n+1}(x_0)]^2}. \quad (A14)$$

(For reasons of convergence we have replaced $\alpha n[n + 1]/\{C_n + \alpha n[n + 1]\} = 1 - C_n/\{C_n + \alpha n[n + 1]\}$ and carried out a partial summation with the aid of Eqs. C1 and C2 from Appendix C.)

Furthermore, from Eqs. A11–A13 we get

$$\frac{4\pi DR}{k_a} = 1 + \beta + (1 - x_0)^{-2}\sum_{1}^{\infty}\frac{P_{n-1}(x_0) - P_{n+1}(x_0)}{C_n + \alpha n(n + 1)}. \quad (A15)$$

Thus, with the explicit expressions for C_n from Eq. A8, ψ_s can be calculated from Eq. A14 and inserted in Eq. A15 to give a closed expression for the effective association rate constant.

APPENDIX B

The association onto a reactive patch on an infinite plane with surface diffusion follows in principle as a special case of the spherical problem discussed above. However, to derive a closed expression for the effective association rate constant, it is more convenient to consider the plane problem separately. Since the basic assumptions and the general procedure of solution is the same as for the spherical case, the discussions below will be very brief. The main difference is a change from spherical coordinates to cylindrical coordinates, and the fact that the infinite plane requires solutions that are integrals rather than sums over eigenfunctions.

Consider a reactive patch ($r < b$, $z = 0$) on an infinite plane surface ($r > b$, $z = 0$), *cf.* Fig. 1. In this case, Eqs. 1–9 of the main text transform to Eqs. B1–B9 below

$$\frac{1}{r}\frac{\partial}{\partial r}\left(r\frac{\partial c}{\partial r}\right) + \frac{\partial^2 c}{\partial z^2} = 0; \qquad z > 0; \quad (B1)$$

$$\frac{D_s}{r}\frac{d}{dr}\left(r\frac{du}{dr}\right) + \phi(r) = 0; \qquad r \geq b; \tag{B2}$$

$$\phi(r) \equiv D\frac{\partial c}{\partial z}\bigg|_{z=0} = \kappa c(r, 0) - \lambda u(r). \tag{B3}$$

The nonspecific binding constant per unit area is

$$K' = \kappa/\lambda. \tag{B4}$$

At infinite distance from the reactive patch

$$\begin{array}{l} c(r, z) \longrightarrow c_0, \qquad u(r) \longrightarrow u_0 = \kappa c_0/\lambda; \\ \quad r \longrightarrow \infty \qquad\quad r \longrightarrow \infty \\ \text{or } z \longrightarrow \infty \end{array} \tag{B5}$$

$$u(r) \equiv 0; \qquad r \leq b; \tag{B6}$$

$$\phi_s \equiv 2\pi\int_b^\infty \phi(r) r dr = 2\pi D_s b\frac{du}{dr}\bigg|_{r=b+}; \tag{B7}$$

$$\phi_d \equiv 2\pi\int_0^b \phi(r) r dr = 2\pi\kappa\int_0^b c(r, 0) r dr; \tag{B8}$$

$$k_a c_0 \equiv \phi_{tot} \equiv \phi_s + \phi_d. \tag{B9}$$

The general solutions can be expressed as

$$c(r, z) = c_0\left[1 - \int_0^\infty A(\xi) e^{-\xi z} J_0(\xi r) d\xi\right]; \tag{B10}$$

$$u_0\left[1 + \int_0^\infty B(\xi) J_0(\xi r) d\xi\right] = \begin{cases} 0; & r \leq b \\ u(r); & r > b. \end{cases} \tag{B11}$$

From these solutions and the closure relation for the Bessel functions (e.g., Arken, 1970, Eq. 11.59), one gets

$$B(\xi) = A(\xi)\,(D\xi/\kappa + 1). \tag{B12}$$

The net flux onto the surface is

$$\phi(r) \equiv D\frac{\partial c}{\partial z}\bigg|_{z=0} = Dc_0\int_0^\infty A(\xi) J_0(\xi r)\,\xi d\xi \tag{B13}$$

valid for all $r \geq 0$. The direct flux onto the reactive patch ($r < b$) can also be expressed as

$$\phi(r) = \kappa c(r, 0) = \kappa c_0\,[1 - \int_0^\infty A(\xi) J_0(\xi r) d\xi]; \quad r < b \tag{B14}$$

and the effective association rate constant from Eq. B9 is

$$k_a \equiv c_0^{-1}\, 2\pi\int_0^\infty \phi(r) r dr = 2\pi D A(0). \tag{B15}$$

Inserting Eq. B11 in Eq. B2 gives

$$-D_s u_0\int_0^\infty B(\xi)\, J_0(\xi r)\,\xi^2 d\xi = \begin{cases} \phi(r); & r > b \\ -(2\pi)^{-1}\phi_s\delta(r - b); & r = b \\ 0; & r < b. \end{cases} \tag{B16}$$

The magnitude of the δ-function contribution at $r = b$ is from Eq. B7

$$\phi_s = 2\pi b D_s u_0\int_0^\infty B(\xi) J_1(\xi b+)\,\xi d\xi. \tag{B17}$$

$B(\xi)$ can be solved from Eq. B16. With Eqs. B12 and B13 the result can be arranged to give for $A(\xi)$

$$2\pi D c_0[1 + (\kappa D_s/\lambda D)\xi + (D_s/\lambda)\xi^2] A(\xi) = \phi_s J_0(\xi b) + 2\pi\int_0^b \phi(r)\, J_0(\xi r) r dr. \tag{B18}$$

Introducing the dimensionless quantities

$$y \equiv r/b, \qquad x \equiv \xi b; \tag{B19a}$$

$$\psi(y) \equiv \pi b^2\phi(r)/\phi_{tot}, \qquad \psi_s = \phi_s/\phi_{tot}; \tag{B19b}$$

$$F(x) \equiv A(\xi)/A(0); \tag{B19c}$$

$$\alpha' \equiv D_s\kappa/\lambda D b, \qquad \beta \equiv D/\kappa b. \tag{B19d}$$

Eqs. B18, B13–B14, and B17 can be expressed, respectively, as

$$(1 + \alpha' x + \alpha'\beta x^2)F(x) = \psi_s J_0(x) + 2\int_0^1 \psi(y) J_0(xy) y dy; \tag{B20}$$

$$2\psi(y) = \int_0^\infty F(x)\, J_0(xy) x dx = \beta^{-1}[2\pi b D/k_a - \int_0^\infty F(x)\, J_0(xy) dx]; \qquad y < 1; \tag{B21}$$

$$\psi_s = \alpha'\int_0^\infty F(x) J_1(x+)\,(\beta x + 1) x dx. \tag{B22}$$

These relations completely determine the problem, and in principle k_a can be solved for. In practice we have to look for suitable approximations.

In the limit when there is no surface diffusion (Shoup et al., 1981), a satisfactory result can be derived from the assumptions that the direct association flux is homogeneous over the reactive patch (i.e., $\psi[y]$ = constant for $y < 1$), and that the absorbing boundary condition, Eq. B21 is satisfied on the average over the patch. Thus let

$$\psi(y) = 1 - \psi_s; \qquad y < 1. \tag{B23}$$

The average of Eq. B21 gives

$$\pi b D/k_a = \int_0^\infty F(x) J_1(x)\,(\beta + 1/x) dx. \tag{B24}$$

Inserting Eq. B23 in B20 gives

$$(1 + \alpha' x + \alpha'\beta x^2)F(x) = 2J_1(x)/(x) - \psi_s J_2(x). \tag{B25}$$

This can be inserted in Eq. B22 to give the fraction ψ_s of ligands associating via surface diffusion

$$\psi_s = \frac{2\alpha'\int_0^\infty \frac{J_1^2(x)(1 + \beta x) dx}{1 + \alpha' x + \alpha'\beta x^2}}{1 - \int_0^\infty \frac{J_1(x)\, J_2(x) dx}{1 + \alpha' x + \alpha'\beta x^2}}. \tag{B26}$$

Inserting Eq. B25 in Eq. B24 finally gives for the effective association rate constant k_a

$$\frac{\pi b D}{k_a} = 2\int_0^\infty \frac{[J_1(x)/x]^2(\beta x + 1) dx}{1 + \alpha' x + \alpha'\beta x^2} - \psi_s\int_0^\infty \frac{[J_1(x)/x]\, J_2(x)(\beta x + 1) dx}{1 + \alpha' x + \alpha'\beta x^2}, \tag{B27}$$

where ψ_s is given by Eq. B26. The first integral dominates this result both for small and large values of the parameter α'.

APPENDIX C

Some sums and integrals over Legendre polynomials employed in the calculations:

$$\sum_{n=1}^{\infty} [P_{n-1}(x) - P_{n+1}(x)]^2/(2n+1) = 1 - x^2; \quad \text{(C1)}$$

$$\sum_{n=1}^{\infty} P_n(x)[P_{n-1}(x') - P_{n+1}(x')] = \begin{cases} x - 1; & x < x' \\ x; & x = x' \\ x + 1; & x > x'; \end{cases} \quad \text{(C2)}$$

$$\sum_{n=1}^{\infty} P_n(x)[P_{n-1}(x') - P_{n+1}(x')]/n(n+1) = \begin{cases} (1+x')\ln\frac{1+x'}{2} - (1-x')\ln\frac{1-x}{2}; & x \le x' \\ (1+x')\ln\frac{1+x}{2} - (1-x')\ln\frac{1-x'}{2}; & x \ge x'; \end{cases} \quad \text{(C3)}$$

$$\sum_{n=1}^{\infty} [P_{n-1}(x) - P_{n+1}(x)]^2/n(n+1)(2n+1) = -(1+x)^2 \ln\frac{1+x}{2} - (1-x)^2 \ln\frac{1-x}{2} - (1-x^2); \quad \text{(C4)}$$

$$\int_0^{\infty} P_n(\cos\theta) P_m(\cos\theta) \sin\theta \mathrm{d}\theta = (n + \tfrac{1}{2})^{-1}\delta_{nm}. \quad \text{(C5)}$$

I thank Dr. Peter von Hippel for his support and many stimulating discussions.

This work was supported by a grant from the Swedish Natural Science Research Council, and by U.S. Public Health Service grant GM 15792 (to P. H. von Hippel, University of Oregon, Eugene, OR).

Received for publication 10 February 1984 and in final form 10 July 1984.

REFERENCES

Adam, G., and M. Delbrück. 1968. Reduction of dimensionality in biological diffusion processes. *In* Structural Chemistry and Molecular Biology. A. Rich and N. Davidson, editors. W. H. Freeman and Co. Publishers, San Francisco. 198–215.

Arfken, G. 1970. Mathematical Methods for Physicists. 2nd ed. Academic Press, Inc., New York. 815 pp.

Barkley, M. D. 1981. Salt dependence of the kinetics of the *lac* repressor-operator interaction: role of nonoperator deoxyribonucleic acid in the association reaction. *Biochemistry.* 20:3833–3842.

Berg, O. G. 1978. On diffusion-controlled dissociation. *Chem. Phys.* 31:47–57.

Berg, O. G, and C. Blomberg. 1976. Association kinetics with coupled diffusional flows. Special application to the *lac* repressor-operator system. *Biophys. Chem.* 4:367–381.

Berg, O. G., and C. Blomberg. 1978. Association kinetics with coupled diffusion III. Ionic-strength dependence of the *lac* repressor-operator association. *Biophys. Chem.* 8:271–280.

Berg, O. G., and M. Ehrenberg. 1982. Association kinetics with coupled three- and one-dimensional diffusion. Chain-length dependence of the association rate to specific DNA sites. *Biophys. Chem.* 15:41–51.

Berg, O. G., R. B. Winter, and P. H. von Hippel. 1981. Diffusion-driven mechanisms of protein translocation on Nucleic Acids. I. Models and theory. *Biochemistry.* 20:6929–6948.

Bloomfield, V. A., and S. Prager. 1979. Diffusion-controlled reactions on spherical surfaces. Application to bacteriophage tail fiber attachment. *Biophys. J.* 27:447–453.

Chou, K. C., and S. P. Jiang. 1974. Studies on the rate of diffusion-controlled reactions of enzymes. Spatial factor and force field factor. *Sci. Sinica.* 27:664–680.

Chou, K. C., and G. P. Zhou. 1982. Role of the protein outside active site on the diffusion-controlled reaction of enzyme. *J. Am. Chem. Soc.* 104:1409–1413.

Fehrst, A. 1977. Enzyme Structure and Mechanism. W. H. Freeman, Co. Publishers, San Francisco. 371 pp.

Hasinoff, B. B. 1982. Kinetics of acetylthiocholine binding to electric eel acetylcholinesterase in glycerol/water solvents of increased viscosity. Evidence for a diffusion-controlled reaction. *Biochim. Biophys. Acta.* 704:52–58.

Hill, T. L. 1975. Effect of rotation on the diffusion-controlled rate of ligand-protein association. *Proc. Natl. Acad. Sci. USA.* 72:4918–4922.

Lepock, J. R., K.-H. Cheng, S. D. Campbell, and J. Kruuv. 1983. Rotational diffusion of TEMPONE in the cytoplasm of Chinese hamster lung cells. *Biophys. J.* 44:405-412.

Richter, P. H., and M. Eigen. 1974. Diffusion-controlled reaction rates in spheroidal geometry. Application to repressor-operator association and membrane-bound enzymes. *Biophys. Chem.* 2:255–263.

Riggs, A. D., S. Bourgeois, and M. Cohn. 1970. The *lac* repressor-operator interaction. III. Kinetic studies. *J. Mol. Biol.* 53:401–417.

Schmitz, K. S., and J. M. Schurr. 1972. The role of orientation constraints and rotational diffusion in bimolecular solution kinetics. *J. Phys. Chem.* 76:534–545.

Schurr, J. M., and K. S. Schmitz. 1976. Orientation constraints and rotational diffusion in bimolecular solution kinetics. A simplification. *J. Phys. Chem.* 80:1934–1936.

Shoup, D., G. Lipari, and A. Szabo. 1981. Diffusion-controlled bimolecular reaction rates. The effect of rotational diffusion and orientation constraints. *Biophys. J.* 36:697–714.

Solc, K., and W. H. Stockmayer. 1971. Kinetics of diffusion-controlled reaction between chemically asymmetric molecules. I. General theory. *J. Chem. Phys.* 54:2981–2988.

Solc, K., and W. H. Stockmayer. 1973. Kinetics of diffusion-controlled reaction between chemically asymmetric molecules. II. Approximate steady-state solution. *Int. J. Chem. Kinet.* 5:733–752.

Sommer, J., C. Jonah, R. Fukuda, and R. Bersohn. 1982. Production and subsequent second-order decomposition of protein disulfide anions. Lengthy collisions between proteins. *J. Mol. Biol.* 159:721–744.

Winter, R. B., O. G. Berg, and P. H. von Hippel. 1981. Diffusion-driven mechanisms of protein translocation on nucleic acids. 3. The *Escherichia coli lac* repressor-operator interaction: Kinetic measurements and conclusions. *Biochemistry.* 20:6961–6977.

Zhou, G. 1979. Influences of van der Waals' force upon diffusion-controlled reaction rate. *Sci. Sinica.* 22:845–858.